

Sintering temperature and composition dependence magnetic properties of $\text{Cu}_{1-x}\text{Mg}_x\text{Fe}_2\text{O}_4$ ferrites

Shahida Akhter^{1*}, M.A. Hakim², S. Manjura Hoque³ and H. N. Das³

¹Department of Physics, University of Chittagong, Chittagong-4331, Bangladesh

²Dept. of Glass and Ceramic Engineering, Bangladesh University of Engineering and Technology, Dhaka

³Materials Science Division, Atomic Energy Centre, Dhaka-1000, Bangladesh.

Abstract: Conventional solid state reaction technique has been used to synthesis of $\text{Cu}_{1-x}\text{Mg}_x\text{Fe}_2\text{O}_4$ ($x=0.2, 0.4, 0.6, 0.8$ and 1.0) ferrites and sintered at $1150^\circ\text{C}, 1175^\circ\text{C}, 1200^\circ\text{C}$ for 2 hours. The effect of different sintering temperatures as well as variation of Mg contents brought applicable changes in the microstructure and magnetic properties of Cu-Mg spinel ferrites. The bulk density, ρ_B and average grain size, D_m increases with increasing sintering temperature for any individual composition. However they are found to decrease with increasing Mg contents for any particular sintering temperature. The real part of permeability, μ' is also found similar trends as in bulk density and grain size. Constant of μ' upto 10 MHz frequency range shows compositional stability and quality of materials. B-H loops indicate the harder ferromagnetic nature by increasing coercivity with increasing Mg contents. The observed features of density, grain size, initial permeability, coercivity and retentivity with sintering temperature as well as Mg contents of the investigated samples has been explained in details in this communication.

Keywords: Ferrites, Solid state reaction, Grain size, Permeability, B-H loop.

I. Introduction

Advancement of science and technology demands tailor-made materials to satisfy requirements of the area of applications. Metallic oxides are an important class of compounds and among them ferrites are most prominent by virtue of the spinel structure. These are preferred because of their high permeability in the radio-frequency (RF) region, high electrical resistivity, mechanical hardness, chemical stability and reasonable cost [1]. Because of these properties, they are widely used in electronics devices, magnetic storage, ferro-fluid technology, catalysis, microwave devices, gas sensors and many bio-inspired applications [2]. Usually ferrites are prepared by the conventional ceramic method that implies a number of stages, including homogenization of the precursor powder, compaction of the reactants and finally prolonged heat treatment at considerably elevated temperatures [3]. These ferrites possessing cubic close-packed structure of oxygen ions are described by the formula $(\text{A})[\text{B}]_2\text{O}_4$ where (A) and [B] represent tetrahedral and octahedral sites respectively. The site occupancy is often depicted in the chemical formula as $(\text{M}_{1-\delta}\text{Fe}_\delta)[\text{M}_\delta\text{Fe}_{2-\delta}]\text{O}_4$ where round and square brackets denote the A- and B-sites, respectively, M represents a metal cation and δ for spinel ferrites is defined as the fraction of tetrahedral (A)-sites occupied by trivalent cations. Accordingly, for a normal spinel $\delta=0$ and for a completely inverse spinel $\delta=1$. The structure, magnetic and electric properties of such a ferrite system depend upon the type of metal cations and their distribution among the two interstitial sites i.e. A- and B-sites [4].

By prominent goodness of magnetic and semiconducting properties, Copper ferrite (CuFe_2O_4) is one of the most ferrites. It undergoes a structural phase transition from tetragonal to cubic accompanied by a reduction in the crystal symmetry to the tetrahedral due to the co-operative Jahn-Teller effect [5]. Mg-based ferrite is pertinent materials because of their high electrical resistivity, low dielectric losses, low cost, high mechanical hardness and environmental stability [6, 7]. With the rapid development of mobile communication and information technology, the electronic devices with small size, low cost and high performance is in demand. As one of the most important surface mounting devices (SMD), multilayer chip inductors (MLCI) made from soft ferrites became more and more miniaturized and integrated. The MLCIs are important components for the latest electronic products such as cellular phones, video cameras, notebook computers, hard and floppy drives, etc which require small dimensions, light weight, and better functions [8, 9,]. There has been a growing interest in Cu-Zn and Cu-Mg ferrites for the applications in producing MLCIs mainly because these oxides can be sintered at relatively low temperatures with a wide range of compositions.

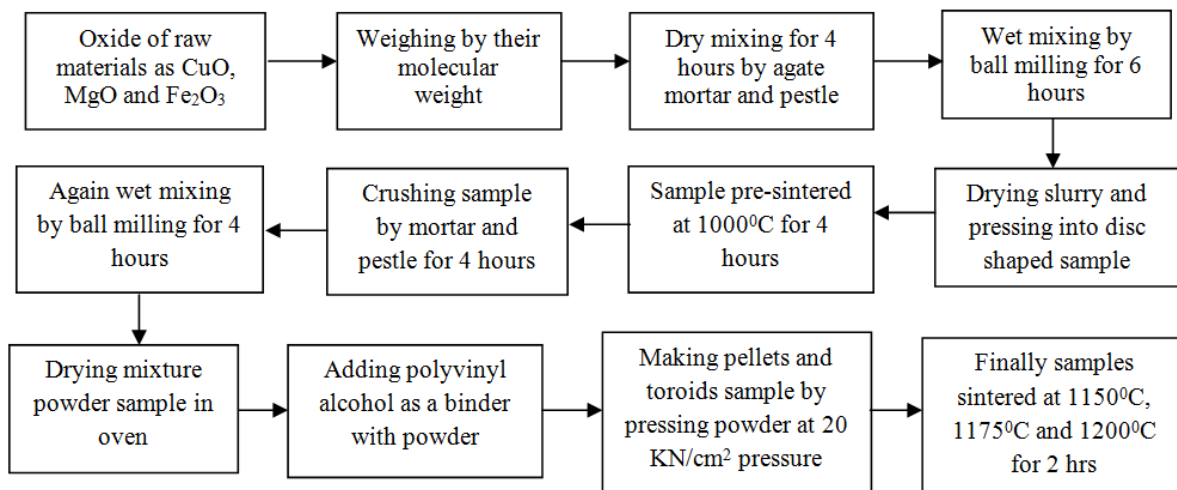
To achieve high permeability, high flux density, low loss and good homogeneous products are apparently highly sensitive to composition and preparation method [10]. Depending on composition and process condition such as sintering temperature and atmosphere leads to change in structural and magnetic properties. In addition magnetic properties depend strongly on the microstructure features such as morphology, grain size and porosity [11]. The present paper deals with systematic study of Mg-substitution in place of Cu-ferrite as well as effect of sintering temperature on magnetic properties of $\text{Cu}_{1-x}\text{Mg}_x\text{Fe}_2\text{O}_4$ ferrite which are prepared by

conventional solid state reaction method. The change of density, grain size, initial permeability, coercivity, retentivity and hysteresis losses with different sintering temperatures and Mg contents of Cu-Mg ferrites were studied and discussed in details.

II. Experimental Procedure

2.1 Preparation Method

Ferrite samples of the chemical formula $Cu_{1-x}Mg_xFe_2O_4$ ($x = 0.2, 0.4, 0.6, 0.8$ and 1.0) were prepared by the double sintering ceramic technique. The preparation procedure of Cu-Mg ferrite comprises of the following operations as shown in the block diagram below:



2.2 Measurement Techniques

The bulk density was calculated by considering the pellet samples and using the relation: $d_B = m/V = m/\pi r^2 h$, where m is the mass, r the radius and h the thickness of the pellet. The microstructures of the sintered ferrites were investigated by a Scanning Electron Microscope (SEM) (Model: FEI Inspect S50). The SEM micrographs were taken on smooth surfaces of the pellet shaped polished samples. The grain size was determined by linear intercept method from surface micrographs of samples. The complex permeability of the toroid shaped samples was measured by the WAYNE KERR Impedance Analyzer (Model: 6500B) at frequency range from 1 kHz to 15 MHz. The real (μ') and the imaginary parts (μ'') of the complex permeability have been determined by using the following relations: $\mu' = (L/L_0)$ and $\mu'' = \mu' \tan \delta$, where L is the measured sample inductance and L_0 is the inductance of the coil of same geometric shape of vacuum. The B-H loop of all samples was measured with Hysteresis Loop Tracer (Laboratorio Elettrofisico AMH-300 B-H loop tracer) for various sintering temperature at constant frequency, $f=1000$ Hz and applied field $H=0-12$ Oe. Different hysteresis parameters such as coercivity (H_c), retentivity (B_r), saturation magnetic flux (B_v), remnant ratio (B_r / B_v), hysteresis losses etc have been obtained from hysteresis curves.

III. Results and Discussion

3.1 Bulk Density

Bulk density is a physical parameter which controls the microstructural and magnetic properties of polycrystalline ferrites. The change of bulk density, ρ_B with sintering temperatures as well as Mg content has been shown in Fig. 1. An increase of bulk density, ρ_B of all samples with increasing sintering temperature from 1150°C to 1200°C is observed in Fig.1. According to Lango and Kellet [12], grain growth and densification are intimately related. The formation of pores within the grain boundaries may be responsible for the increase in density with increasing sintering temperature. During the sintering process, the thermal energy generates a force to grow the grain boundary over pores. In this observation, bulk density also increase due to increase of grain boundary with increasing sintering temperatures. Shahida et. al. [6] also found in increase of density with increasing sintering temperature from 950°C to 1050°C for Zn substitution in Cu-Zn ferrites. Similar increase in density with increasing sintering temperature from 850°C to 950°C for Mg substituted NiCuZn ferrites by Hua et. al. [13]. It is also observed from Fig. 1 that with increasing Mg content, bulk density gradually decrease for every sintering temperature. This might be explained on the basis of the atomic weight of substituted cations and density of constituent ferrites. The atomic weight of Mg (24.31 emu) is less than that of Cu (63.55 emu) and as well as the density of $MgFe_2O_4$ (4.512 g/cm^3) is smaller than $CuFe_2O_4$ (5.4 g/cm^3) [14]. By incorporation of

small atomic weight and density of Mg in the system decrease the density. Similar decrease in density with increasing Zn content in $\text{Cu}_{1-x}\text{Zn}_x\text{Fe}_2\text{O}_4$ ferrites has been observed by Shahida et. al. [15].

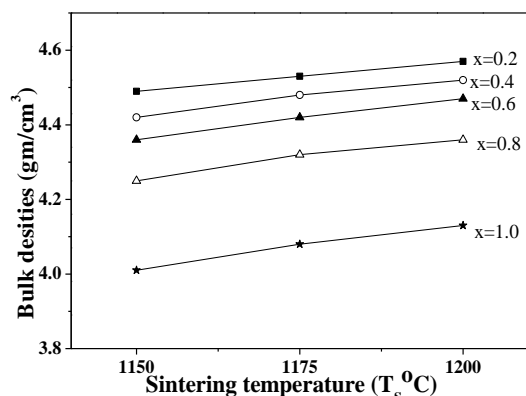


Fig. 1: Variation of bulk density with sintering temperature.

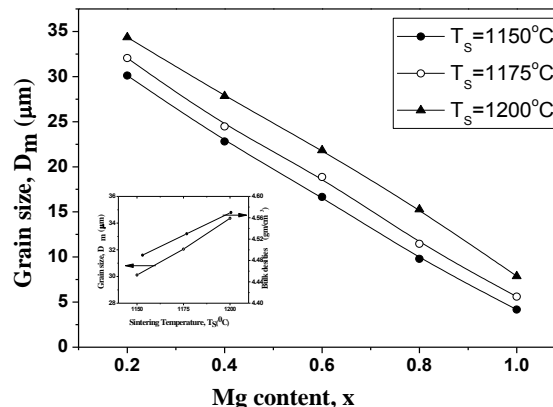


Fig. 2: Change of grain size with Mg content.

3.2 Grain Size

Microstructural analysis determines the average grain size and the type of grain growth of the samples, which influence the magnetic properties of the materials. Average grain sizes of the samples are determined from the micrographs by the linear intercepts techniques. Change of average grain size of all samples of Cu-Mg ferrites with different sintering temperature has been illustrated in Fig. 2. It is noticed that, average grain size declines with increasing Mg content for a particular sintering temperature. This decreasing trend in grain size can be attributed as MgO plays a role as a microstructural stabilizer which is responsible for finer and uniform grain size [16]. Also MgO is a stable oxide avoids presence of divalent ion and thereby prevents tendency of discontinuous grain growth [17]. Moreover decrease of grain size could be due to increase of intra-granular porosity since the pores neutralize the driving force and the thickness of the grain boundary is found to increase which leads to decrease the grain size. Grain size decreases also due to the reaction condition, which favoured the formation of new nuclei preventing further growth of particles [18]. Similar decrease in grain size with increasing Mg content in $\text{Zn}_{1-x}\text{Mg}_x\text{Fe}_2\text{O}_4$ ferrites by Oaigle et. al. [19].

Increasing grain size with increasing sintering temperature is clearly evident in Fig. 2 for all samples. The average grain size increase 30.11 μm to 35.78 μm for sample $x=0.2$ and similar pattern for other samples at sintering temperature increasing from 1150°C to 1200°C. Higher grain size for all samples at higher sintered temperature at 1200 °C may be attributed to the formation of Fe^{2+} ions, which accelerate the growth rate of grains [20]. This decrease also may be due to the facts that during sintering process, the grain boundaries become larger by driving/capillary forces which are generated by thermal energy. The strength of driving/capillary forces depends upon the diffusing of individual grains, sintering temperature and porosity. The inter-granular porosity increased due to increase of sintering temperature which is capable of moving with a grain boundary leading to grain growth. Increase of average grain size is also increase of bulk density with increasing sintering temperature which is shown in inset of Fig. 2. High sintering temperature which helps to grow large grains plays an important role for magnetic properties such as the permeability [21]. Similar increase of grain growth with sintering temperatures has been predicted by Manjurul et. al. in Mg-Cu-Zn ferrites [22].

3.3 Complex Permeability

Complex permeability spectra (real part μ' and imaginary part μ'') for Cu-Mg ferrites sintered at 1200°C has been presented in Fig. 3 (a and b). From Fig. 3, it is noticed that real part of initial permeability, μ' remain stable upto 16 MHz for sample $x=0.8$ and $x=1.0$ and upto 10 MHz for samples $x=0.2, 0.4, 0.6$ for all sintering temperatures. Similar observation was found at sintering temperatures 1150°C and 1175°C which was not shown in Fig. At higher frequency >10 MHz, permeability falls slightly to lower values at where there is an increase in imaginary part of permeability. At higher frequency >16 MHz, sharply fall of permeability for all samples might be observed clearly, but our experimental limitation was upto 16 MHz. The measurements of permeability suggest that the frequency spectrum in the frequency range of investigation is due to relaxation process and the permeability mechanism arises mainly due to the domain wall displacement. In the present system, constant of permeability upto 10 MHz is due to relaxation process and permeability mechanism due to displacement of the domain walls. Beyond 10 MHz the rotation of magnetization starts taking place indicating a contribution to permeability from the resonance phenomena. These fairly constant values of μ' over a certain frequency range

show compositional stability which is suitable for different applications such as broadband pulse transformers and wide band read-write heads for video recording [23].

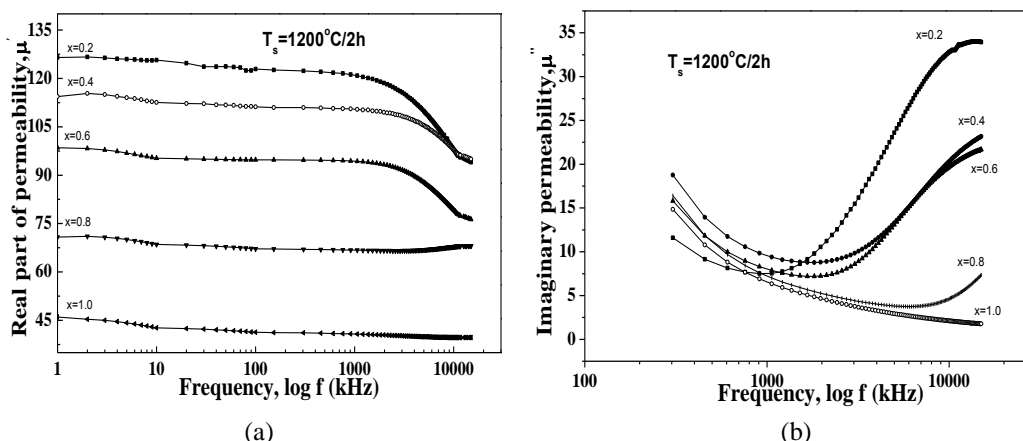


Fig. 3: (a) Real and (b) Imaginary part of permeability at $T_s=1200^\circ\text{C}$.

The frequency at which μ' attains maximum value and after that decrease is known as resonance frequency f_r . The f_r is the limiting frequency of magnetic materials below which the materials can be efficiently used. From Fig. 3 (a), it is also observed that μ' decrease whereas f_r increase with increasing Mg content for a particular temperature which is desired properties of ferrites. At sintering temperature 1150°C , f_r value increase with value 1.3, 2.2 and 3.5 MHz whereas the value of μ' decrease with value of 96, 87 and 62 for sample $x=0.2$, 0.4 and 0.6. Similar pattern of variation of μ' and f_r observes in other sintering temperature. This inversely proportional relation of μ' and f_r confirms Snoek's limit, $\mu' f_r = \text{constant}$ [24]. Fig. 4 shows the variation of μ' and f_r for sample $x=0.4$ with sintering temperatures. From Fig. 4, it is also observed that resonance frequency f_r shifts to lower value whereas permeability to higher value with increasing sintering temperature. Similar pattern also observed in sample $x=0.2$ and 0.6 which is not shown in Fig. 4. It is well know that relaxation frequency of domain wall oscillation is inversely proportional to grain diameter [25]. From our observation, it is also found that relaxation frequency decreases whereas grain size increases with increasing sintering temperatures which confirms inverse relationship as state in ref. [25].

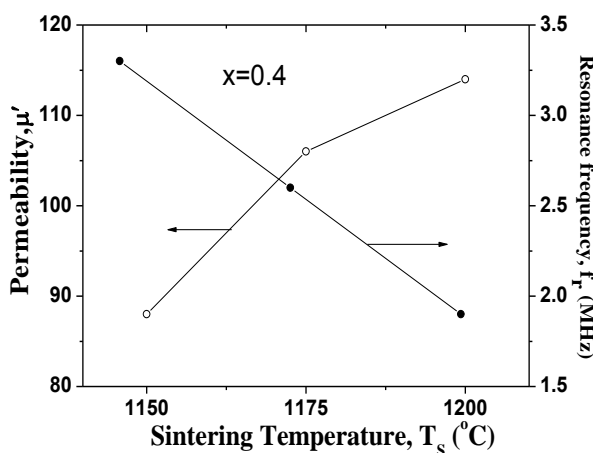


Fig. 4: Variation of permeability and resonance frequency with sintering temperature for $x=0.4$.

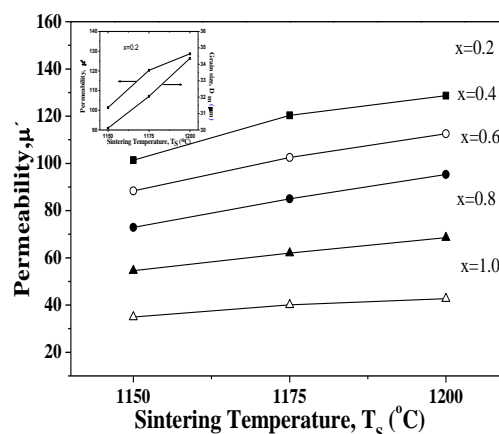


Fig.5: Variation of Permeability with sintering temperatures (permeability with grain size in insert).

Fig. 5 shows permeability μ' increases with increasing sintering temperature for a particular composition as well as decrease with increasing Mg content for a particular sintering temperature. This can be attributed to the increase in density and grain size with increasing sintering temperature (also shown in insert). Increase of sintering temperature facilitates the movement of spins so the number of pores reduces the wall motion. Higher density and grain size leads to higher permeability due to higher sintering temperature. The increase in temperature also decreases magnetic anisotropy by decreasing internal stress, resulting increased the value of permeability [26]. Generally, a higher initial permeability is achieved through the control of both the

density and microstructure, which depends on the sintering temperatures. The decreasing trend in μ' with increasing Mg content can be attributed to the decrease in grain size. According to Globus relation [27], permeability is directly proportional to the grain size. Decrease of number of domain walls in each grain occurs due to decrease of grain size. As the movement of domain walls determines the initial permeability, so decrease of grain size leads to decrease in permeability [28].

3.4 B-H loop

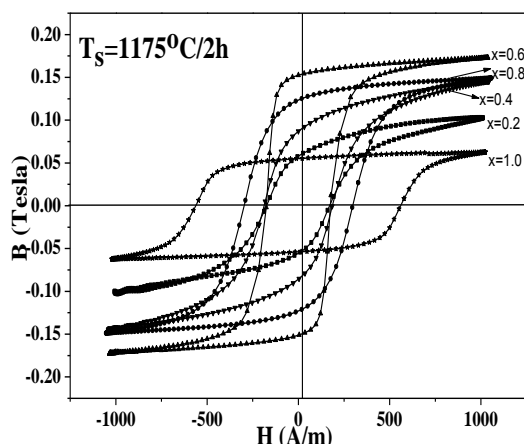


Fig. 6: B-H loop for all samples at $T_s=1175^\circ\text{C}$.

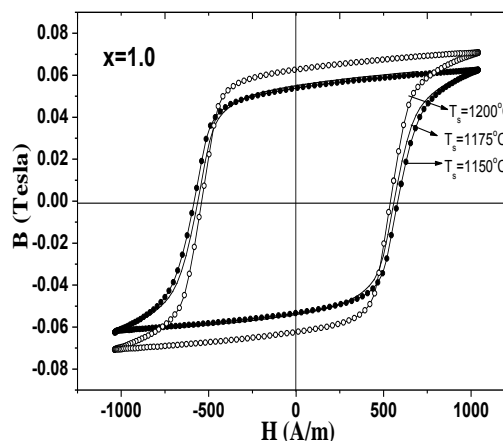


Fig. 7: B-H loop for $x=1.0$ at different sintering temperatures.

Magnetic hysteresis loop (B-H loop) serves as a finger print proof for determining the ordering of spins in magnetic materials. Fig. 6 shows hysteresis loop for all compositions at sintering temperature 1175°C whereas Fig. 7 shows hysteresis loop at different sintering temperatures for sample $x=1.0$. The magnetic properties such as coercivity (H_c), retentivity (B_r), hysteresis loss were elucidated from hysteresis loop and given in Table with permeability values at different sintering temperatures. From Fig. 7, it is noticed that loop area increases with increasing Mg content from $x=0.2$ to 1.0 and loop area decreases with increasing sintering temperatures is observed in Fig. 7. Increase of Loop area with increasing Mg content indicates the sample reducing its softer ferromagnetic nature. Decrease of loop area with increasing sintering temperatures can be attributed due to increase of grain size with increasing sintering temperatures.

Table: Magnetic parameters at different sintering temperatures of Cu-Mg ferrites

Mg content x	Permeability, μ'			Coercivity, H_c (Oe)			Retentivity, B_r (Tesla)			Power loss (W/Kg)		
	1150 °C	1175 °C	1200 °C	1150 °C	1175 °C	1200 °C	1150 °C	1175 °C	1200 °C	1150 °C	1175 °C	1200 °C
0.2	101.34	120.29	128.65	2.343	2.071	1.883	0.828	0.658	0.567	15.67	13.16	11.60
0.4	88.33	102.54	112.54	2.53	2.304	2.104	1.195	1.138	0.988	24.01	20.41	18.47
0.6	72.93	85.03	95.27	3.123	2.752	2.443	1.426	1.269	0.972	32.56	28.51	24.94
0.8	54.61	62.01	68.53	4.29	3.737	3.47	1.167	1.032	0.954	39.21	36.26	33.79
1.0	34.94	40.10	42.68	7.316	7.053	6.782	0.639	0.605	0.545	45.81	41.83	39.68

Coercivity of the materials or coercive force, H_c is defined as the amount of reverse magnetic field which must be applied to magnetic materials to make flux return to zero. The coercivity is influenced by factor such as anisotropy constant, density, grain size and magnetic domain. The coercivity of all samples at different sintering temperatures has been plotted in Fig. 8 which shows coercivity decreases with increasing sintering temperatures while increases with increasing Mg content. This decrease in H_c may be due to an increase in density and grain size with increasing sintering temperatures. Larger grains tend to consist of more magnetic domains, so for the rotation of these domains need small energy. So samples with larger grains are expected to have low coercivity. Similar decrease in coercivity with increasing sintering temperatures has been observed by Ponhan et. al. in $CuFe_2O_4$ [29] and by Li et. al. in $NiFe_2O_4$ [21]. Cullity [30] has given a relationship between H_c and grain size in which H_c is inversely proportional to grain by using this equation $H_c = a + \frac{b}{D}$ where a & b are constants. Iagarashi [31] and Gabal [32] have shown through the experimental and theoretical derivations that H_c is inversely propositional to the grain size. In present system, coercivity increase with increasing Mg content due to the predominance of decrease of grain size which also confirms the Culliyt's proposed relation.

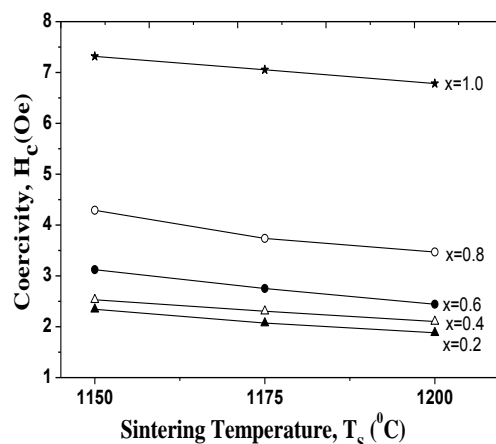


Fig. 8: Coercivity at different sintering temperatures.

The magnetic remanence or retentivity (B_r) of a magnetic material is the degree of residual magnetization when the saturation magnetic field (H) is reduced to zero. From Table, it is found that B_r values decrease with increasing sintering temperatures from 1150°C to 1200°C. This can be attributed to decrease of anisotropy constant K_1 with increase of sintering temperatures. Hysteresis losses are very useful information from the application point of view. The values of hysteresis loss are 15.67, 13.16, 11.60 W/Kg for $x=0.2$ and 45.81, 41.83, 39.68 W/Kg for $x=1.0$. For other samples similar variation is also observed in Table. It is found that hysteresis loss is increasing with increasing Mg content and decreases as sintering temperature increase. The area within the hysteresis loops is directly related to the hysteresis loss. So the increase of Mg content significantly influence the area of the hysteresis curve, they cause a enhancement of the coercive field which turn lead to a increase in the loop area and hence to a increase in the hysteresis losses.

IV. Conclusions

The experimental results we present above are intended to describe the effect of sintering temperatures as well as Mg content on the physical and magnetic properties of $\text{Cu}_{1-x}\text{Mg}_x\text{Fe}_2\text{O}_4$ ($x = 0.2, 0.4, 0.6, 0.8$ and 1.0) ferrites. In case of physical parameters, bulk density and grain size increase with increase of sintering temperatures whereas decrease with increase of Mg content. Maximum bulk density and largest grain size were found at highest sintering temperature 1200°C. Permeability μ' is found to increase with increasing sintering temperature and decrease with increasing Mg content. Resonance frequency f_r has been greatly influenced by sintering temperatures and Mg contents. Increase of μ' and decrease of f_r values with sintering temperatures suggested the Snoek's relation. According to Globus, a linear relation between permeability and grain size observed in studied samples. From B-H loop study, coercivity, retentivity and hysteresis loss decrease with increasing sintering temperatures while increase with increasing Mg content. The inverse relation between coercivity and grain size was observed according to Cullity's suggestions.

Acknowledgement

The author (Shahida Akhter) is grateful to Materials Science Division, Atomic Energy Centre (AECD), Dhaka, Bangladesh for using its laboratory facilities to prepare the samples and to carry out the experimental measurement.

References

- [1]. T. Nakamura, 'Snoek's limit in high frequency permeability of polycrystalline Ni-Zn, Mg-Zn and Ni-Zn-Cu spinel ferrites' *J. Appl. Phys.*, 88 (No.1), 2000, 348-353.
- [2]. Z.L. Wang, Y. Liu, Z. Zhang, 'Handbook of nanophase and nano-structured materials', vol. 3, New York: Kluwer Academic/Plenum Publishers, 2000.
- [3]. V. Berbenni, A. Marin, C. Milanese, G. Bruni, 'Solid state synthesis of CuFe_2O_4 from $\text{Cu}(\text{OH})_2 \cdot \text{CuCO}_3 \cdot 4\text{Fe}_2\text{O}_3 \cdot 2\text{H}_2\text{O}$ mixture: mechanism of reaction and thermal characterization of CuFe_2O_4 ' *J. Ther. Anal. Calorim.*, 99, 2011, 437-442.
- [4]. R. Valenzuela, 'Magnetic Ceramics', Cambridge University Press, Cambridge, 1994.
- [5]. S. Manjura Hoque, Md. Ammanullah Choudhury, Md. Fakrul Islam, 'Characterization of Ni-Cu mixed spinel ferrites' *J. Magn. Magn. Matt.*, 251, 2002, 292-303.
- [6]. Xiwei Qi, Ji Zhou, Zhenxing Yue, Zhilum Gui, Longtu Li, 'Effect of Mn substitution on the magnetic properties of MgCuZn ferrites' *J. Magn. Magn. Matt.*, 251, 2002, 316.
- [7]. M.A. El Hiti, 'Dielectric behaviour in Mg-Zn ferrites' *J. Magn. Magn. Matt.*, 192, 1999, 305.
- [8]. A. Ono, T. Muruno, N. Kaihara, 'Development of Non-Shrinking Soft Ferrite Composition Useful for Microinductors Applications' *Jpn. Electron. Eng.*, 28, 1991, 5.
- [9]. T. Nomura, A. Nakano, Proceedings of ICF-6, Japan Society of Powder and Powder Metallurgy, 1992, 1198.

- [10]. A.A. Sattar, H.M. El-Sayed, K.M. El-Shokofy, M.M. El-Tabey, 'Improvement of Magnetic properties on Mn-Ni-Zn ferrites by non-magnetic Al^{3+} Ion Substitution' *J. Appl. Sci.*, 5(1), 2005, 162.
- [11]. A.K. Singh, T.C. Goel, R.G. Mendiratta, 'Effect of cation distribution on the properties of $Mn_{0.2}Zn_xNi_{0.8-x}Fe_2O_4$ ' *Solid State Commun.*, 125, 2003, 121.
- [12]. R.F. Lange, B.J. Kellert, 'Powder Processing Science and Technology for Increased Reliability' *J. Am. Ceram. Soc.*, 72, 1989, 735.
- [13]. Hua Su, Huaiwu Zhang, Xiaoli Tang, Yulan Jing, Baoyuan Liu, 'Electromagnetic properties of Mg substituted NiCuZn Ferrites for Multilayer Chip inductors Application' *IEEE Trans. Mg.*, 45(No. 5), 2009, 2050-2052.
- [14]. M. Ammanullah Chowdhury, J. Rahman, 'Magnetic and electrical properties of $(Ni_{0.8}Cu_{0.2})_{1-x}Co_xMn_{0.02}Fe_{1.9}O_4$ ferrites' *J. Magn. Magn. Matt.*, 223, 2001, 21-26.
- [15]. Shahida Akhter, Deba Prasad Paul, Md. Abdul Hakim, Dilip Kumar Saha, Md. Al Mamun, Alhamra Parveen 'Synthesis, Structural and Physical Properties of $Cu_{1-x}Zn_xFe_2O_4$ ferrites' *Materials Sciences and Applications (MSA)* 2, 2011, 1675-1681.
- [16]. E. Rezlescu, N. Rezlescu, P.D. Popa, L. Rezlescu, C. Pasnicu, M.L. Craus, 'Effect of copper oxide content on intrinsic properties of MgCuZn ferrite' *Mater. Res. Bull.*, 33(6), 1998, 915.
- [17]. Narla Varalaxmi, N. Ramamanohar Reddy, Madinepalli Venkata Ramasa, Eyunni Rajagopal, V. Ramakrishna Murthy, Kota Venkata Sivakumar, 'Stress sensitivity of inductance in NiMgCuZn ferrites and development of a stress insensitive ferrite composition for microinductors' *J. Mater. Sci.:Mater. Electron*, 19, 2008, 399-404.
- [18]. Muhammad A., Maqsood A., 'Structural, electric and magnetic properties of $Cu_{1-x}Zn_xFe_2O_4$ ferrites ($0 \leq x \leq 1$)' *J. Alloy. Compds.*, 460, 2008, 54-59.
- [19]. A. Daigle, J. Modest, A.L. Geiler, S. Gillelte, Y. Chen, M.Geiler, B. Hu, S. Kim, K. Stopher, C. Villoria, V.G. Harris, "Structure, morphology and magnetic properties of $Mg_{(x)}Zn_{(1-x)}Fe_2O_4$ ferrites prepared by polyol and aqueous co-precipitation methods: a low-toxicity alternative to $Ni_{(x)}Zn_{(1-x)}Fe_2O_4$ ferrites," *Nanotechnology*, 22, 2011, 305708.
- [20]. Anjali Verma, Ratnamala Chatterjee, 'Effect of zinc concentration on the structural, electric and magnetic properties of mixed Mn-Zn and Ni-Zn ferrites' *J. Magn. Magn. Matt.*, 306, 2006, 313-320.
- [21]. Li Lv, Jian-Ping Zhou, Qian Liu, gang-giang Zhu, Xian-Zhi Chen, Xiao-Bing Bian, Peng Liu, 'Grain size effect on the dielectric and magnetic properties of $NiFe_2O_4$ ceramics' *Physica E*, 43, 2011, 1798-1803.
- [22]. M. Manjurul Hoque, M. Huq, M.A. Hakim, 'Influence of Cu and sintering temperature on the microstructure and magnetic properties of Mg-Cu-Zn ferrites' *J. Magn. Magn. Matt.*, 320 (2008) 2792-2799.
- [23]. Gangon Kumar, Jagdish Chand, Anjana Durga, P.K. Kotnala, M. Sing, 'Improvement in electrical and magnetic properties of mixed Mg-Al-Mn ferrite system synthesized by citrate precursor technique' *J. Phy. Chem. Solids*, 71, 2010, 375-380.
- [24]. J.L. Snoek, 'Dispersion and absorption in magnetic ferrites at frequencies above one Mc/s' *Physica*, 14, 1948, 207.
- [25]. A. Goldman, 'Handbook of Modern Ferromagnetic Materials' Kluwer Academic Publishers, Boston, USA, 1999.
- [26]. Su-Ho Kang, Han-III Yoo, 'The effect of nonstoichiometry (δ) on the magnetic properties of $(Mg_{0.22}Mn_{0.07}Fe_{0.71})_{3-\delta}O_4$ ferrite' *J. Appl. Phys.*, 88, 2000, 4754.
- [27]. A. Globus, P. Duplex, *IEEE Trans. On Magnetics, MGM-2*, 1966, 441-445.
- [28]. A.K.M. Akther Hossain, T.S. Biswas, Takeshi Yanagida, Hidekazu Tanaka, Hishoshi Tabata, Tomoji Kawai, 'Investigation of structural and magnetic properties of polycrystalline $Ni_{0.50}Zn_{0.50-x}Mg_xFe_2O_4$ spinel ferrites' *Mater. Chem. Phys.*, 120, 2010, 461-467.
- [29]. Wichaid Ponhan, Santi Maensiri, 'Fabrication and magnetic properties of electrospun copper ferrite ($CuFe_2O_4$) nanofibers' *Solid State Science*, 119, 2009, 479-484.
- [30]. B.D. Cullity, C.D. Graham, 'Introduction to Magnetic Materials', *IEEE Press*, 2nd ed. Wiley (2009).
- [31]. H. Igarashi, K. Okazaki, 'Effect of porosity and grain size in magnetic properties of Ni-Zn ferrites' *J. Am. Ceram. Soc.*, 60(1-2), 1977, 51.
- [32]. M.A. Gabal, 'Effect of Mg substitution on the magnetic properties of NiCuZn ferrite nanoparticles prepared through a novel method using egg white' *J. Magn. Magn. Mater.*, 321 (2009) 3144-3148.